REPORT DOCUMENTATION PAGE

Form Approved
OMB No. 0704-0188

1. AGENCY USE ONLY (*Leave Blank*)	2. REPORT DATE 01/18/00	3. REPORT TYPE AND DATES COVERED FINAL: 01 MAY 96 through 30 SEPTEMBER 99

4. TITLE AND SUBTITLE
Very High Frequency Mode-Stabilized VCSELs for Linear/RF Photonic Applications

5. FUNDING NUMBERS
FDN00014-96-1-0583

6. AUTHORS
PROFESSORS CONNIE CHANG-HASNAIN AND KAM LAU

7. PERFORMING ORGANIZATION NAME(S) AND ADDRESS(ES)
THE REGENTS OF THE UNIVERSITY OF CALIFORNIA, BERKELEY
C/O SPONSORED PROJECTS OFFICE
336 SPROUL HALL
BERKELEY, CA 94720-5940

8. PERFORMING ORGANIZATION REPORT NUMBER

9. SPONSORING / MONITORING AGENCY NAME(S) AND ADDRESS(ES)
OFFICE OF NAVAL RESEARCH
BALLSTON CENTRE TOWER ONE
800 NORTH QUINCY STREET
ARLINGTON, VA 22217-5660

10. SPONSORING / MONITORING AGENCY REPORT NUMBER

11. SUPPLEMENTARY NOTES

12a. DISTRIBUTION / AVAILABILITY STATEMENT
APPROVED FOR PUBLIC RELEASE

12b. DISTRIBUTION CODE

13. ABSTRACT *(Maximum 200 words)*

Vertical cavity surface emitting lasers (VCSELs) have emerged as a key optical source in digital and RF photonics systems. Investigation to date has involved VCSELs of "standard" DBR construction. However, incorporation of a controllable saturable absorber inside the lasing cavity results in a wealth of new dynamic characteristics.

The focus of this program is on designs and experiments of a novel three contact verical cavity laser with an intracavity quantum-well. Contrary to all existing laser-absorber integration we achieved an independent control of the gain region and the quantum-well absorber. This allowed the device to be used as an integrated optical source and modulator, or alternatively, providing nonlinearity for self-pulsation and optical feedback. An unprecendentedly wide range of application is made possible with the unique properties and flexibilities.

Under this program we graduated 3 PhD students, one post-doctoral researcher and one MS student. The grant also helped to start several new students. We published over 20 publications, filed one patent application and presented 12 invited talks at international conferences. This invention brought forth a completely new class of VCSELs. Many other research organizations have followed our lead and published their new designs and inputs. We believe the impact of this work is a far-reaching one.

14. SUBJECT TERMS
VCSEL, vertical cavity surface emitting lasers, semiconductor diode lasers, optical communications, RF Photonics

15. NUMBER OF PAGES
31

16. PRICE CODE

17. SECURITY CLASSIFICATION OF REPORT	18. SECURITY CLASSIFICATION OF THIS PAGE	19. SECURITY CLASSIFICATION OF ABSTRACT	20. LIMITATION OF ABSTRACT
UNCLASSIFIED	UNCLASSIFIED	UNCLASSIFIED	UL

NSN 7540-01-280-5500

Standard Form 298 (Rev. 2-89)
Prescribed by ANSI Std. Z39-1
298-102

ONR CONTRACT NUMBER N00014-96-1-0583

VERY HIGH FREQUENCY MODE-STABILIZED VCSELS FOR LINEAR/RF PHOTONIC APPLICATIONS

PRINCIPAL INVESTIGATOR: PROF. C. J. CHANG-HASNAIN

CO-INVESTIGATOR: PROF. KAM LAU

DEPT. OF ELECTRICAL ENGINEERING AND COMPUTER SCIENCE
UNIVERSITY OF CALIFORNIA
BERKELEY, CA 94720

1. Abstract

Vertical cavity surface emitting lasers (VCSELs) have emerged as a key optical source in digital and RF photonics systems. Investigation to date has involved VCSELs of "standard" DBR construction. However, incorporation of a controllable saturable absorber inside the lasing cavity results in a wealth of new dynamic characteristics.

The focus of this program is on designs and experiments of a novel three-contact vertical-cavity laser with an intracavity quantum-well. Contrary to all existing laser-absorber integration, we achieved an independent control of the gain region and the quantum-well absorber. This allowed the device to be used as an integrated optical source and modulator, or alternatively, providing nonlinearity for self-pulsation and optical feedback. An unprecedented wide range of applications is made possible with the unique properties and flexibilities.

Under this program, we graduated 3 PhD students, one post-doctoral researcher and one MS student. The grant also helped to start several new students. We published over 20 publications, filed one patent application and presented 12 invited talks at international conferences. This invention brought forth a completely new class of VCSELs. Many other research organizations have followed our lead and published their new designs and inputs. We believe the impact of this work is a far-reaching one.

2. Overview

We have designed and fabricated a novel VCSEL with a quantum well (QW) absorber integrated into the upper mirror stack. The three-contact design of this structure enables independent control of the gain and absorber regions. Furthermore, our three-contact vertical cavity laser offers an additional degree of design flexibility that is not available in the analogous edge-emitters. Because the lasing wavelength of a VCSEL is determined simply by the optical cavity length, the position of the lasing wavelength relative to the absorber bandedge of our three-contact device can be precisely controlled. Exploiting this flexibility, we have executed two distinct designs for our structures, leading to novel device physics and a wide range of applications.

In the full-length technical report, we describe the design and fabrication of the two types of our device. We show that if our three-contact VCSEL is designed such that the lasing wavelength is shorter than the absorber bandedge, then the absorber exhibits broad negative differential resistance. We attribute this phenomenon to variations in the cavity photon density in response to changes in the relative absorption. If instead the laser is designed such that the lasing wavelength is slightly longer than the absorber bandedge, sharp negative differential resistance arises in the absorber.

Four different system applications arise from such design variations: low-chirp optical intensity modulation, independent control of amplitude and phase modulation, high-frequency self-pulsation, and a monolithic optical pick-up. The applications are all described in the report.

3. Summary of Major Accomplishments

- Developed VCSEL with active intracavity absorber:
  - Designed absorber to select device behavior
  - Determined origin of negative differential resistance
- First demonstration of controllable multi-GHz self-pulsating VCSELs. Achieved controllable self-pulsation: pulses up to 2 GHz, tuned over 700 MHz
- First demonstration of high speed modulation at 9 GHz with reduced frequency chirp and low-noise phase modulation
- First demonstration of bistable VCSEL and its application as a compact, integrated optical pickup device

4. Students Supported By This Program

Former students:	Sui F. Lim, PhD 1998 Now at Agilent
	W. Yuen, PhD 1999 Now at Bandwidth9 Inc.
	Rob Stone, Postdoc, 1999 Now at Bandwidth9 Inc.
	Janice Hudgings, PhD 1999 Now at Mount Holyoke College
	Steve Chase, MS 2000 Now at Johns Hopkins University
Current Students:	Lukas Chrostowski, Chih-Hao Chang, Jacob Hernadez, P. C. Ku

5. Publications

1) J.A. Hudgings, R.J. Stone, S.F. Lim, G.S. Li, W. Yuen, K.Y. Lau, and C.J. Chang-Hasnain, "The Physics of Negative Differential Resistance of an Intracavity Voltage-Controlled Absorber in a Vertical Cavity Surface Emitting Laser," Applied Physics Letters, 73 (13), p.1796-1798, 1998.

2) J.A. Hudgings, S.F. Lim, G.S. Li, W. Yuen, K.Y. Lau, and C.J. Chang-Hasnain, "Compact, Integrated Optical Disk Readout Head using a Novel Bistable Vertical Cavity Surface Emitting Laser," *Photonics Technology Letters*, 1998.

3) J.A. Hudgings, S.F. Lim, G.S. Li, W. Yuen, K.Y. Lau, and C.J. Chang-Hasnain, "Self-Pulsations, Bistability, and Intracavity Quantum Well Absorber Modulation of VCSELs," in *Optoelectronic Integrated Circuits II, Proceedings of the SPIE*, vol. 3290, ed. S. Wang and Y. Park, 1998.

4) J.A. Hudgings, R.J. Stone, C.H. Chang, S.F. Lim, K.Y. Lau, and C.J. Chang-Hasnain, "Dynamic Behavior and Applications of a Three-Contact Vertical Cavity Surface Emitting Laser," *IEEE Journal of Selected Topics in Quantum Electronics*, June, 1999.

5) R.J. Stone, J.A. Hudgings, C.H Chang, K.Y. Lau, and C.J. Chang-Hasnain, "Independent Phase and Magnitude Control of an Optically Carried Microwave Signal with a Three Terminal Vertical Cavity Surface Emitting Laser," *Photonics Technology Letters*, accepted for publication, 1998.

6) S.F. Lim, J.A. Hudgings, L.P. Chen, G.S. Li, W. Yuen, K.Y. Lau, and C.J. Chang-Hasnain, "Novel Intracavity Modulator Integrated with a Vertical-Cavity Surface-Emitting Laser," in *Trends in Optics and Photonics Series (TOPS)*, ed. C.J. Chang-Hasnain, Washington, D.C., Optical Society of America, 1997, vol. 15, p.48-52, 1997.

7) S.F. Lim, J.A. Hudgings, G.S. Li, W. Yuen, K.Y. Lau, and C.J. Chang-Hasnain, "Self-Pulsating and Bistable VCSEL with Controllable Intracavity Quantum-Well Saturable Absorber," *Electronics Letters*, 33 (20), p.1708-9, 1997.

8) S.F. Lim, J.A. Hudgings, L.P. Chen, G.S. Li, W. Yuen, K.Y. Lau, and C.J. Chang-Hasnain, "Modulation of a Vertical-Cavity Surface-Emitting Laser using an Intracavity Quantum-Well Absorber," *IEEE Photonics Technology Letters*, 10 (3), p.319-321, 1997.

9) S.F. Lim, J.A. Hudgings, G.S. Li, W. Yuen, K.Y. Lau, and C.J. Chang-Hasnain, "VCSELs with a Novel Integrated Quantum-Well Absorber," in *Vertical-Cavity Surface-Emitting Lasers II, Proceedings of the SPIE*, vol. 3286, ed. R.A. Morgan and K.D. Choquette, 1998.

10) S. F. Lim, G. S. Li, W. Yuen, and C. J. Chang-Hasnain, "Vertical Cavity Lasers with an Intracavity Quantum Well Detector," Electronics Letters, Vol. 33, 7, 27 March, 1997.

11) J.A. Hudgings, R.J. Stone, C.H Chang, K.Y. Lau, and C.J. Chang-Hasnain, "Integrated Phase and Magnitude Control of a Microwave Optical Subcarrier Using a Three-Contact Vertical Cavity Surface Emitting Laser with an Intracavity Absorber," (accepted), *1999 Optical Fiber Communication Conference*, San Diego, CA, February 1999.

12) J.A. Hudgings, S.F. Lim, R.J. Stone, G.S. Li, W. Yuen, K.Y. Lau, and C.J. Chang-Hasnain, "Applications and Device Physics of a Novel VCSEL with an Intracavity Quantum-Well Absorber," *OSA Annual Meeting*, Baltimore, MD, October 1998.

13) J.A. Hudgings, S.F. Lim, G.S. Li, W. Yuen, K.Y. Lau, and C.J. Chang-Hasnain, "Frequency Tuning of Self-Pulsations in a VCSEL with a Voltage-Controlled Saturable Absorber," *1998 Optical Fiber Communication Conference*, San Jose, CA, February 1998.

14) J.A. Hudgings, S.F. Lim, G.S. Li, W. Yuen, K.Y. Lau, and C.J. Chang-Hasnain, "Self-Pulsations, Bistability, and Intracavity Quantum Well Absorber Modulation of VCSELs," *SPIE Photonics West Optoelectronics Integrated Circuits Conference*, San Jose, CA, January 1998.

15) R.J. Stone, J.A. Hudgings, S.F. Lim, G.S. Li, K.Y. Lau, and C.J. Chang-Hasnain, "Negative Differential Resistance of an Intracavity Voltage-Controlled Absorber in a Vertical Cavity Surface Emitting Laser," 16th IEEE International Semiconductor Laser Conference, Nara, Japan, October 1998.

16) S. F. Lim, G. S. Li, W. Yuen, and C. J. Chang-Hasnain, "Intracavity Quantum-Well Photodetection of a Vertical-Cavity Surface-Emitting Laser," 15th IEEE International Semiconductor Laser Conference (ISLC'96), Haifa, Israel, 13-18 Oct. 1996.

17) S. F. Lim, L. P. Chen, G. S. Li, W. Yuen, K. Y. Lau, and C. J. Chang-Hasnain, "Novel Intracavity Modulator Integrated with a Vertical-Cavity Surface-Emitting Laser," Conference on Lasers and Electro-Optics (CLEO'97), Baltimore, MD, 18-23 May 1997, paper CWA3.

18) S.F. Lim, J.A. Hudgings, G.S. Li, W. Yuen, K.Y. Lau, and C.J. Chang-Hasnain, "Self-Pulsating VCSEL with Controllable Quantum-Well Saturable Absorber," *IEEE/LEOS'97 Summer Topical Meetings*, Montreal, Quebec, Canada, August 1997.

19) S.F. Lim, J.A. Hudgings, G.S. Li, W. Yuen, K.Y. Lau, and C.J. Chang-Hasnain, "Novel Bistable VCSEL for Efficient and Compact Optical Pickup Applications," *CLEO'98*, San Francisco, CA, May 1998.

20) S.F. Lim, J.A. Hudgings, G.S. Li, W. Yuen, K.Y. Lau, and C.J. Chang-Hasnain, "VCSELs with a Novel Integrated Quantum-Well Absorber," *SPIE Photonics West Optoelectronics Integrated Circuits Conference*, San Jose, CA, January 1998.

6. Patents

- S.F. Lim, J.A. Hudgings, K.Y. Lau, and C.J. Chang-Hasnain, "Design Criteria Of A Vertical Cavity Surface Emitting Laser For Self-Pulsations, Intracavity Absorber Modulation, And Optical Pick-Up Detection," US Patent Application filed May 1997

7. Technology Transfer

- Patent Application licensed by Bandwidth9 Inc. Fremont California

FINAL REPORT

ONR CONTRACT NUMBER N00014-96-1-0583

PROGRAM TITLE:

VERY HIGH FREQUENCY MODE-STABILIZED VCSELS FOR LINEAR/RF PHOTONIC APPLICATIONS

DURATION: 5/1/96 TO 9/30/99

SUBMITTED BY

PRINCIPAL INVESTIGATOR

PROF. C. J. CHANG-HASNAIN
571 CORY HALL
DEPT. OF ELECTRICAL ENGINEERING AND COMPUTER SCIENCE
UNIVERSITY OF CALIFORNIA
BERKELEY, CA 94720
TEL: (510) 642-4315
FAX: (510) 643-7345
EMAIL: CCH@EECS.BERKELEY.EDU

CO-INVESTIGATOR

PROF. KAM LAU
DEPT. OF ELECTRICAL ENGINEERING AND COMPUTER SCIENCE
UNIVERSITY OF CALIFORNIA
BERKELEY, CA 94720
EMAIL: KLAU@EECS.BERKELEY.EDU

TABLE OF CONTENTS

Executive Summary

Vertical cavity surface emitting lasers (VCSELs) have emerged as a key optical source in the digital optical communication domain as well as in RF photonics systems. Investigation to date has involved VCSELS of "standard" DBR construction. However, incorporation of a controllable saturable absorber inside the lasing cavity results in a wealth of new dynamic characteristics which can be exploited in many useful RF signal processing and transmission functions. This report describes results of a detailed experimental and theoretical investigation of the properties of such a VCSEL device.

The focus of this program is on designs and experiments of a novel three-contact vertical-cavity laser with an intracavity quantum-well. Because of the additional absorbing layer, this laser exhibits unusual device physics. Contrary to all existing laser-absorber integration, we achieved an independent control of the gain region and the quantum-well absorber. This allowed the device to be used as an integrated optical source and modulator, or alternatively, providing nonlinearity for self-pulsation and optical feedback.

An unprecendentedly wide range of applications is made possible with the unique properties and design flexibility offered by our three-contact, vertical-cavity laser with an intracavity absorber. We executed two distinct designs for our structures, leading to novel device physics and a wide range of applications, including low-chirp modulator-laser integration, QAM, bistable laser and self-pulsating laser.

Under this program, we graduated 3 PhD students, one post-doctoral researcher and one MS student. The grant also helped to start several new students. As the research scope became far wider than we initially anticipated, we are fortunate to be able to leverage the support from another ONR grant, MURI-RF Photonics program lead by UCLA. We published over 20 publications and presented about a dozen invited talks in international conferences.

This invention deserves more research work to fully exploit the opportunity brought forth by this new class of VCSELs we have started. In fact, other research organizations, e.g. Sandia National Labs and Tokyo Institute of Technology, have already followed our lead and published their new designs and inputs. We believe the impact of this work is an exceedingly far-reaching one.

Introduction

We have designed and fabricated a novel VCSEL with a quantum well (QW) absorber integrated into the upper mirror stack. The three-contact design of this structure enables independent control of the gain and absorber regions. Furthermore, our three-contact vertical cavity laser offers an additional degree of design flexibility that is not available in the analogous edge-emitters. Because the lasing wavelength of a VCSEL is determined simply by the optical cavity length, the position of the lasing wavelength relative to the absorber bandedge of our three-contact device can be precisely controlled. Exploiting this flexibility, we have executed two distinct designs for our structures, leading to novel device physics and a wide range of applications.

In Section 2, we describe the design and fabrication of the two types of our device. We show that if our three-contact VCSEL is designed such that the lasing wavelength is shorter than the absorber bandedge, then the absorber exhibits broad negative differential resistance. We attribute this phenomenon to variations in the cavity photon density in response to changes in the relative absorption. If instead the laser is designed such that the lasing wavelength is slightly longer than the absorber bandedge, sharp negative differential resistance arises in the absorber.

Four different system applications arise from such design variations: low-chirp optical intensity modulation, independent control of amplitude and phase modulation, high-frequency self-pulsation, and a monolithic optical pick-up. The applications are described in section 3 to 4.

Section 5 concludes and discusses future work. In Section 6, we lists all graduate students and scholars who were involved in this program and Section 7 lists all the publications resulted from the support of this program.

1. Design Criteria

1.1 Baseline Design

Our novel device is a vertical cavity surface emitting laser with an n-p-n configuration that has an additional quantum well integrated into the upper mirror stack, as shown in Figure 2.1.

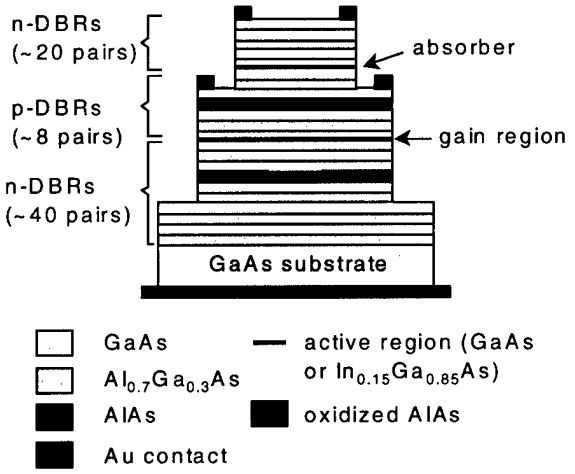

Figure 2.1. Device schematic.

A distributed Bragg reflector (DBR) mirror composed of n-doped $Al_{0.7}Ga_{0.3}As$ and GaAs pairs is grown on a GaAs substrate. A single 3λ/4 AlAs oxidation layer is included in this DBR stack. This mirror is followed by the gain region, comprised of a 1-λ thick $Al_{0.35}Ga_{0.65}As$ spacer which contains either two 80 Å $In_{0.15}Ga_{0.85}As$ quantum wells or three 70 Å GaAs quantum wells. An p-doped DBR stack with another 3λ/4 AlAs oxidation layer is grown on top of the gain region, followed by a 5λ/4 spacer with a single 80 Å $In_{0.15}Ga_{0.85}As$ quantum well or a 90 Å GaAs quantum well. This second active region is followed by an n-doped DBR mirror. During fabrication, the double mesa structure is obtained by dry etching, the two AlAs layers are exposed to wet thermal oxidation, and annular gold contacts are deposited as shown in Figure 2.1.

The n-p-n configuration of our VCSEL allows independent biasing of the two active regions. The lower multiple quantum well active region is forward biased to serve as the gain region, while the second, single-quantum well active region acts as an intracavity absorber under reverse bias. The two oxide layers improve the current and modal confinement of the device while inhibiting lasing in "oxide modes."

Typical CW lasing characteristics for our Design are shown in Figure 2.2. At 300 K with 0 V applied across the absorber section, the lasing threshold current of the device measured in Figure 2.2 is 1.7 mA, corresponding to a threshold current density of 1.8 kA/cm^2. At the lasing threshold, the voltage across the gain region is 5.6 V. The maximum output power of our devices ranges from 0.7-1 mW.

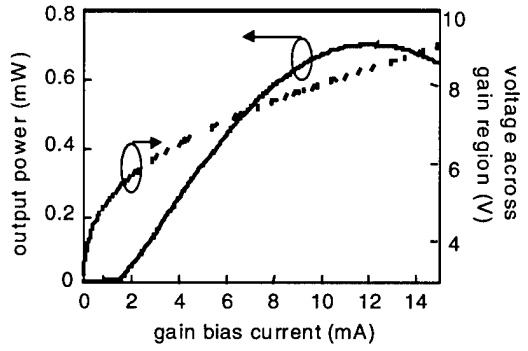

Figure 2.2. Typical CW lasing characteristics measured at 300 K, with 0 V applied across the absorber section.

The unique design flexibility of our VCSEL enables precise control of the relative positions of the lasing wavelength and absorber bandedge. Due to the characteristic short cavity length of a VCSEL, the lasing wavelength of our device is determined by the single Fabry-Perot mode which falls within the gain spectrum. Hence, the lasing wavelength can be precisely engineered by controlling the optical cavity length. To fully exploit this flexibility, we have fabricated devices with two distinct designs. In Design A, the lasing wavelength is designed to be shorter than the absorber bandedge. In Design B, the lasing wavelength is slightly longer than the absorber bandedge. As expected, the behavior of our device is strongly dependent on the position of the lasing wavelength relative to the absorber bandedge.

1.2 Broad Negative Differential Resistance (Design A)

In Design A, the lasing wavelength is shorter than the absorber bandedge. The lasing wavelength at twice the threshold injection current density is 829 nm, whereas the ground state excitonic peak of the absorber is positioned at 852 nm. The absorber in this device is a single 90 Å GaAs quantum well. The gain region is composed of three 70 Å GaAs quantum wells with the gain peak at 843 nm.

The current versus voltage (I-V) characteristic of the absorber in Design A is shown in Figure 2.3. The absorber in this Design Acts much like a standard photodetector, with the measured photocurrent increasing relatively linearly with increasing optical power in the cavity.

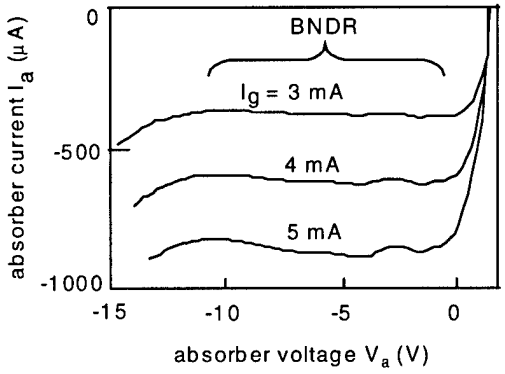

Figure 2.3. Experimental data of absorber current versus voltage (I_a-V_a) characteristics in a typical Design A, whose lasing wavelength is shorter than the absorber bandedge. The traces, each measured with a different DC gain bias current (I_g), exhibit broad negative differential resistance (BNDR).

The broad region of negative differential resistance (BNDR) in the absorber characteristic arises due to variations in the cavity photon density in response to changes in the relative absorption; the origin of this phenomenon is shown schematically in Figure 2.4. The dashed curves in Figure 2.4 show the response of a typical photodiode; the solid line shows the response of our intracavity absorber. When the absorber is biased as shown in Region 1 (Figure 2.4), the absorber acts like a typical photodiode in the presence of the lasing photons. Applying a small reverse bias to the absorber (Region 2) causes increased absorption and hence a reduction in the cavity photon density, which has the net effect of reducing the absorber photocurrent. Under a strong reverse bias voltage (Region 3), the absorption is so large that the device ceases to lase, so the absorber behaves like a standard photodiode with very little incident optical power. Hence, it is this trade-off between the strength of the absorber and the cavity photon density which causes the BNDR in the absorber characteristic of Design A.

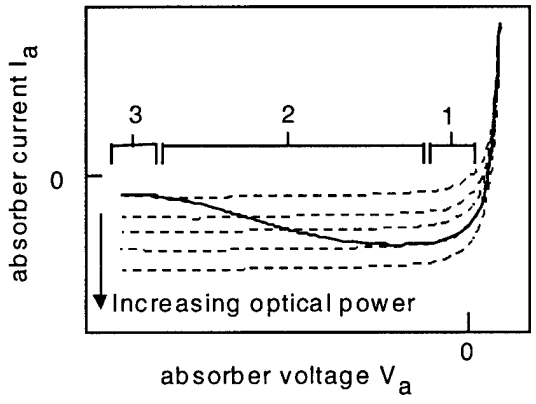

Figure 2.4. Schematic illustrating the origin of broad negative differential resistance in the absorber I_a-V_a traces of Design A. Dashed lines show the response of a typical external photodiode; solid line shows the response of the intracavity absorber.

1.3 Sharp Negative Differential Resistance (Design B)

In contrast, the lasing wavelength of Design B is slightly longer than the absorber bandedge. The lasing wavelength at twice the threshold injection current density is 959 nm, and the ground state excitonic peak of the absorber is positioned at 948 nm. The absorber is a single 80 Å $In_{0.15}Ga_{0.85}As$ quantum well. The gain region in this device is composed of two 80 Å $In_{0.15}Ga_{0.85}As$ quantum wells with the gain peak at 940 nm.

The absorber I-V characteristic of Design B is shown in Figure 2.5. With this device design, a region of sharp negative differential resistance (SNDR) occurs in absorber I-V. We attribute this behavior to Stark-shifting of the ground-state absorption excitonic peak across the lasing wavelength.

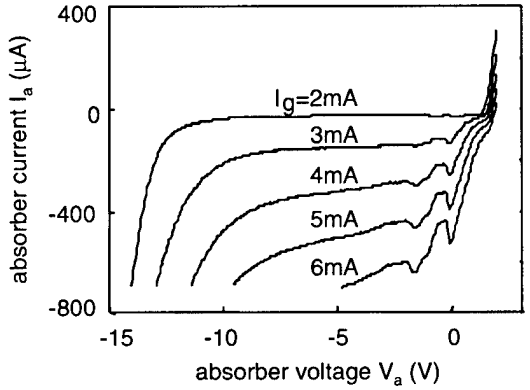

Figure 2.5. Absorber current versus voltage (I_a-V_a) characteristics for Design B, in which the lasing wavelength is longer than the absorber bandedge. The traces, each measured with a different DC gain bias current (I_g), exhibit sharp negative differential resistance (SNDR).

The measured absorption spectra for Design B are shown in Figure 2.6. Again, the ground state absorption excitonic peak Stark shifts with applied absorber bias voltage. We have modeled the expected shift in the absorption bandedge due to QCSE, using the techniques given in [1.9] with a 2400 Å long intrinsic region and a built-in voltage of 1.4 V.

If the wavelength of the injected light from the Ti-Sapphire probe laser is fixed at 940 nm (corresponding to the vertical line in Figure 2.6), then the absorber I-V characteristic, with no applied gain bias, exhibits SNDR as shown in Figure 2.7. The origin of this SNDR is illustrated by Figures 2.6 and 2.7. The absorber photocurrent is a maximum when the excitonic peak coincides with the 940 nm wavelength of the injected light; this occurs at an absorber bias voltage (V_a) of 0.5V. As the reverse bias voltage is increased, the absorber photocurrent diminishes as the excitonic peak is Stark shifted away from 940 nm.

In order to extend this logic to explain the SNDR observed in the absorber when our device is lasing (Figure 2.5), the effects of the greatly increased cavity photon density must be considered. In the "cold cavity" measurements of Figures 6 and 7, in which our device is not lasing, the injected optical power is estimated to be on the order of 1 mW. However, when the device is lasing, the optical power in the cavity is on the order of 500 mW. The two-orders-of-magnitude increase in the cavity photon density when the device is lasing necessitates the inclusion of both carrier heating and carrier screening effects to explain its behavior.

Heating of the optical cavity at lasing powers causes red shifting of both the Fabry-Perot mode and of the gain and absorption spectra. At a 6 mA gain current bias, the CW lasing wavelength of Design B is 959.3 nm, which is 0.5 nm longer than the lasing wavelength under pulsed operating conditions (958.8 nm). Since the Fabry-Perot wavelength of a VCSEL has been shown to shift by 0.6 Å/°C and the absorption spectrum of bulk InGaAs shifts by 3 Å/°C, we estimate from the shift

in lasing wavelength that with a 6 mA gain bias, the absorber bandedge redshifts by about 2 nm due to heating.

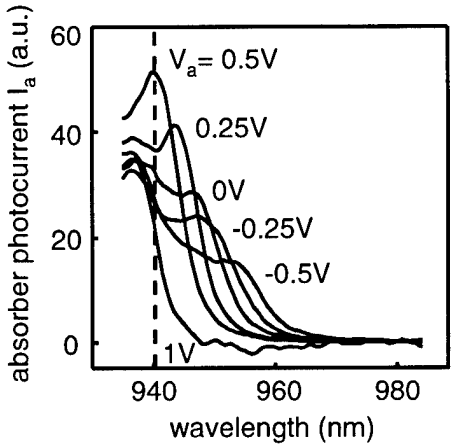

Figure 2.6. Solid lines show measured absorption spectra for Design B, with varying absorber bias voltages (V_a) and zero gain bias current. Intersections between dashed line and absorption spectra give the relative absorption of light at 940 nm.

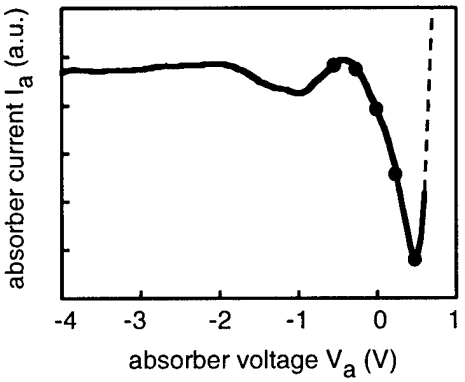

Figure 2.7. Absorber I_a-V_a characteristic with 1 mW of 940 nm light injected from an external source. Gain bias current is zero. The dots correspond to the intersections in Figure 2.6 between the dashed line and the absorption spectra.

In addition, carrier screening causes band gap shrinkage of the absorber when the device is lasing. From the measured absorber photocurrent and a calculated carrier escape time of 10 ps, we estimate that at a gain bias current of 6 mA there are approximately $10^{11}/cm^2$ carriers in the absorber quantum well. With this carrier density, we expect a band gap shrinkage of 10 meV, which causes a 7.5 nm red shift in the absorption spectrum.

If the absorption spectrum when the laser is operated at a gain bias current of 6mA is red shifted by the expected 9.5 nm relative to the "cold cavity" case, then we expect the absorption excitonic peak with no applied absorber bias to occur at 957.5 nm. Since the lasing wavelength of Design B is about 959 nm, the absorption excitonic peak will be Stark shifted across the lasing wavelength with applied absorber bias voltage, thereby sweeping out the SNDR observed in Figure 2.5.

2. Applications For Design A

In this section, we present applications for Design A, which is ideal for use as an intracavity optical modulator. Optical intensity modulation using this technique is shown to provide bandwidth and modulation efficiencies comparable to those obtained with direct gain modulation, while potentially reducing the frequency chirp. Use of our three-contact device for integrated generation and modulation of a microwave optical subcarrier enables independent control of both the phase and magnitude of the subcarrier.

2.1 Direct Optical Intensity Modulation

The ability to modulate vertical-cavity lasers at high frequencies is essential for data transmission applications. While direct gain modulation of VCSELs can be used to obtain reasonably large (GHz) modulation bandwidths, this technique is ultimately limited by frequency chirping and intrinsic parasitics [1, 2, 3]. Alternatively, an external modulator can be used to modulate the output power of a VCSEL without causing frequency chirping. However, this technique requires a long interaction length in order to achieve sufficient modulation depth, resulting in a cumbersome bulk. We demonstrate an alternative scheme in which the modulation signal is applied to the intracavity absorber of our novel VCSELs. By applying the modulation to our quantum-well absorber, which is located inside the optical cavity at a peak of the optical intensity distribution, we achieve high-speed modulation (9 GHz) and a high modulation efficiency (7 GHz/$\sqrt{}$mA) with a single quantum well. Furthermore, small signal analysis of the laser rate equations predicts that at high modulation frequencies, absorber modulation causes less frequency chirp than does direct gain modulation [4, 5, 6].

The modulation speed of our absorber modulation technique was measured using the biasing circuitry shown in Figure 3.1. The gain region is biased with a simple DC current source, and a 50 Ω termination path is provided for any AC current arising in the gain region as the device is modulated. The absorber is reverse biased with a DC voltage source in parallel with a small-signal AC voltage modulation.

The response of the device to absorber modulation is shown in Figure 3.2, for a variety of gain bias conditions. We achieve a small signal modulation bandwidth of 9 GHz at a gain bias current of 8 mA and a modulation depth of 0.6%. As expected, the small-signal modulation bandwidth increases as the square root of the gain current bias above threshold. The bandwidth efficiency of the absorber modulation technique (7 GHz/$\sqrt{}$mA) is shown in Figure 3.3 to be comparable to that obtained using direct gain modulation. Furthermore, the absorber modulation bandwidth is relatively independent of the choice of DC absorber bias; see Figure 3.4.

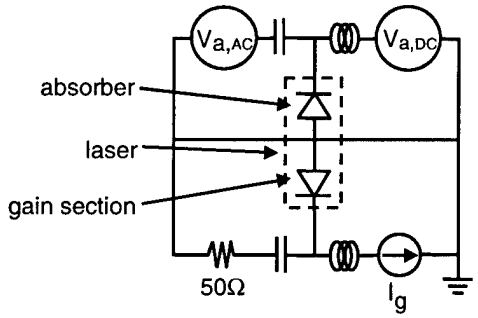

Figure 3.1. Biasing circuitry used for direct optical carrier modulation by small signal modulation of the intracavity absorber.

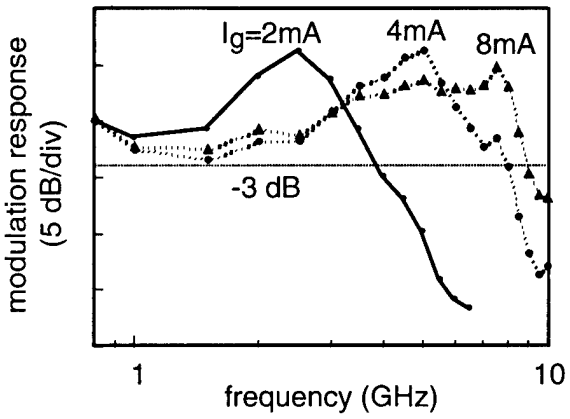

Figure 3.2. Absorber modulation response for varying DC gain bias currents (Ig). The DC absorber bias Va,DC = 1 V, and the small-signal AC modulation of the absorber voltage is -10 dBm.

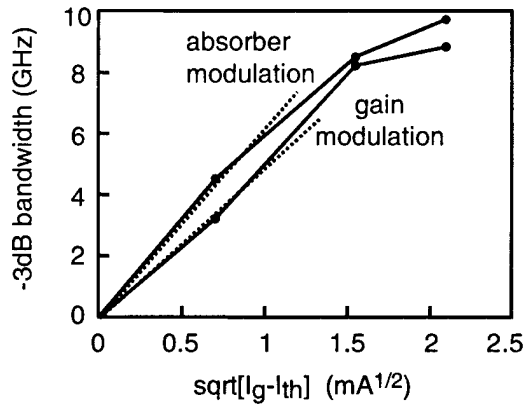

Figure 3.3. Bandwidth efficiency of absorber modulation compared to gain modulation. The slope efficiency (dashed line) is 7 GHz/√mA for absorber modulation and 5 GHz/√mA for gain modulation. Bias conditions for this measurement are $V_{a,DC}$ = 1 V and $V_{a,AC}$ = -10 dBm.

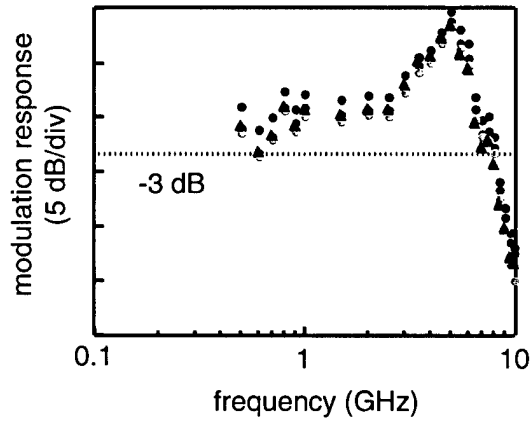

Figure 3.4. Absorber modulation response for fixed DC gain bias currents (I_g = 4 mA) and varying DC absorber biases ($V_{a,DC}$). The small-signal AC modulation of the absorber voltage is -10 dBm.

2.1.1 Modeling of Frequency Chirp

The frequency chirp due to intracavity absorber modulation is compared in the following discussion to the chirp introduced by conventional direct current modulation [6].

Modulating the absorber effectively modulates the mirror loss since the absorber is part of the VCSEL mirror stack. This in turn leads to modulation of the photon lifetime, which causes variations in both the cavity photon density and the carrier density of the gain region. We use a small signal analysis of the rate equations (see also [7] for standard rate equations) to compare the frequency chirp due to intracavity absorber modulation ($\delta\tau_p$, where τ_p is the photon lifetime) to the chirp obtained using direct current modulation (δJ, where J is the injected current density). Define δn_γ to be the change in the carrier density of the gain region when the absorber is modulated (i.e. $\delta J = 0$). Likewise, define δn_J to be the change in the carrier density of the gain region when the pump current is modulated (i.e. $\delta\tau_p = 0$). The ratio of the two, $|\,\delta n_\gamma / \delta n_J\,|$, provides a comparison of the chirp produced by the two techniques. Note that this ratio depends on the modulation frequency ω:

$$\frac{\delta n_\gamma}{\delta n_J} = -\frac{\left(v_g g + S v_g \frac{\partial g}{\partial S}\right)\left(S v_g \Gamma \frac{\partial g}{\partial n} + 2\Gamma\beta_{sp} Bn\right)}{\left(i\omega + \frac{1}{\tau_{\Delta e}} + S v_g \frac{\partial g}{\partial n}\right)\left(i\omega - \Gamma v_g g + \frac{1}{\tau_p} - S v_g \Gamma \frac{\partial g}{\partial S}\right)} \qquad (1)$$

where v_g = group velocity, S = photon density, g = gain, Γ = confinement factor, β_{sp} = spontaneous emission factor, $\tau_{\Delta e} = (A+2Bn+3Cn^2)^{-1}$, A = nonradiative recombination coefficient, B = radiative recombination coefficient, and C = Auger recombination coefficient.

The magnitude of the two-pole response given by (1) monotonically decreases with ω due to the heavy damping introduced by $\partial g/\partial S$ and $\partial g/\partial n$. For frequencies greater than f_C (the frequency at which $|\,\delta n_\gamma/\delta n_J\,| = 1$), absorber modulation produces less chirp than direct modulation. From equation (1):

$$\omega_c = 2\pi f_c \approx \sqrt{S v_g \Gamma \frac{\partial g}{\partial n}\left(v_g g + S v_g \frac{\partial g}{\partial S}\right)} \approx \sqrt{\omega_R^2 + S^2 v_g^2 \Gamma \frac{\partial g}{\partial n}\cdot\frac{\partial g}{\partial S}} \qquad (2)$$

where ω_R is the resonance frequency. Since $\partial g/\partial S$ is negative, f_C is less than the resonance frequency. Figure 3.5 shows the calculated effect of absorber and gain modulation on the carrier density in the gain region for the same photon modulation depth and standard VCSEL parameters [7]. From Figure 3.2, the ratio of the -3dB-frequency f_{-3dB} to f_C is 1.6, so the critical frequency occurs well within the useful bandwidth of the device. Hence, absorber modulation at frequencies between f_C and f_{-3dB} results in less chirp than does direct gain modulation.

The carrier density within the absorber layer is also modulated. However, the absorber is far away from the active region, so any frequency chirping effects should be quite small.

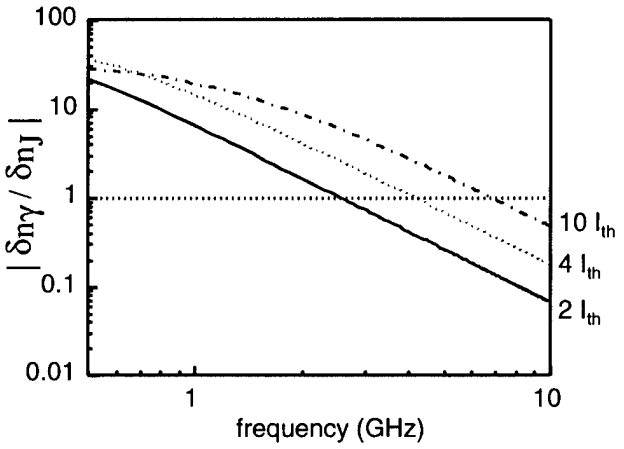

Figure 3.5. Predicted effect of absorber and direct modulation on carrier density in the gain region. When $|\delta n_\gamma| < |\delta n_J|$, absorber modulation results in less chirp than does direct gain modulation.

2.1.2 Discussion of Design Criteria

The relative placement of the gain peak wavelength (λ_{gain}), the absorption peak wavelength (λ_{abs}), and the Fabry-Perot transmission peak wavelength (λ_{FP}) is an important design criterion for this device. Ideally, we should have $\lambda_{gain} < \lambda_{FP}$ in order to achieve maximum overlap of the gain peak with the Fabry-Perot as the gain peak red-shifts with increasing pump current. Furthermore, we desire that $\lambda_{abs} < \lambda_{FP}$ with these two wavelengths fairly close to each other, so that a small change in the applied voltage across the absorber induces a large change in the absorption due to the quantum-confined Stark effect. Since the wavelength of the pumped gain region will shift further than will the wavelength of the voltage-biased absorber, the ideal relative positioning of the three wavelengths should be $\lambda_{gain} < \lambda_{abs} < \lambda_{FP}$.

In contrast, if the ideal conditions are not met, we expect a reduction in modulation efficiency and speed. Placing the Fabry-Perot wavelength too much longer than the peak wavelength of the gain or absorber leads to poor modulation efficiency since greater voltages across the absorber are required to sweep the absorption edge across the Fabry-Perot wavelength [4]. Furthermore, the smaller overlap of the gain peak with the Fabry-Perot results in a narrow bandwidth [4].

In the device used for the experimental measurements, the Fabry-Perot wavelength (828 nm) is shorter than that of the gain (~843 nm) or absorber quantum well (~ 851 nm). In this case, changing the absorber DC bias does not result in a significant change in the absorption or the modulation response, as shown in Figure 3.4.

We expect that aligning the Fabry-Perot wavelength to be redder than the absorber quantum-well band edge will result in excellent modulation depth with this absorber modulation technique. A reverse bias across the absorber can then be used to sweep the absorption edge across the laser emission, resulting in a very high on-off ratio. Future work will include optimization of the bandwidth, growth and fabrication for large-signal modulation, and single-mode operation to demonstrate low frequency chirp.

2.2 Microwave Optical Subcarrier Modulation

In systems with limited bandwidth, combinations of phase and amplitude modulation such as quadrature amplitude modulation (QAM) may be utilized to maximize the achievable bit rate. Generating phase and amplitude modulated signals for use in an optical system typically requires modulating an external microwave electrical signal with the required amplitude and phase, which is then used to modulate the optical source. We demonstrate a novel integrated arrangement, in

which the phase and magnitude of a GHz-range optical intensity modulation of our three-contact VCSEL can be independently controlled by applying DC voltage and current biases to the VCSEL. In addition to applications in QAM optical data transmission, this device could also be used as an optical driver for phased antenna arrays [8, 9, 10].

A schematic of the biasing circuitry is shown in Figure 3.6. The three-contact, n-p-n configuration of our VCSEL allows independent control of the active absorber and gain regions. A GHz-range optical subcarrier is obtained by biasing the gain region above threshold with a DC current source ($I_{g,DC}$) and applying a small-signal modulation ($I_{g,DC}$, typically ~ -10dBm) with constant phase and amplitude to the gain region. The phase and amplitude of the resulting optical subcarrier can be independently controlled by varying the DC bias points of the gain current and absorber voltage.

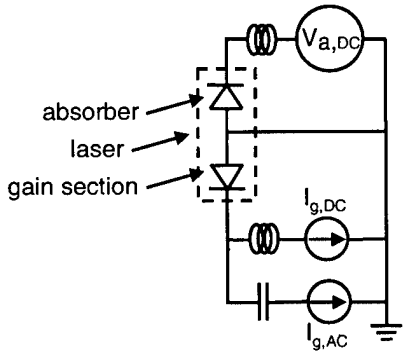

Figure 3.6. Biasing circuit used for phase and amplitude control of three-contact VCSEL.

The origin of the phase and amplitude variation of the subcarrier as the DC biases of the gain and absorber are varied can be understood qualitatively from the standard two-pole model of small-signal modulation of a semiconductor laser [7]. With this model, the relaxation oscillation frequency is given by $\omega_R = (1/\tau_p\, v_g\, dg/dn\, P_0)^{1/2}$, where τ_p is the photon lifetime, v_g is the group velocity, dg/dn is the variation of the gain with the carrier density, and P_0 is the steady-state photon density. Increasing the DC gain bias current increases the relaxation oscillation frequency and, for bias currents sufficiently close to threshold, reduces the damping of the response, as shown in Figures 2.7a and 2.7b. Varying the absorber bias voltage alters the magnitude of the absorption as discussed in Section 1 [11], hence changing both the photon lifetime and the steady state photon density. The resulting small changes in both the relaxation oscillation frequency and the damping of the small-signal modulation response cause shifts in both the magnitude and phase of the subcarrier, as shown schematically in Figure 3.7b. Figure 3.7c shows a schematic of the resulting phase shift between the high and low loss conditions used in Figures 2.7a and 2.7b, as a function of subcarrier frequency.

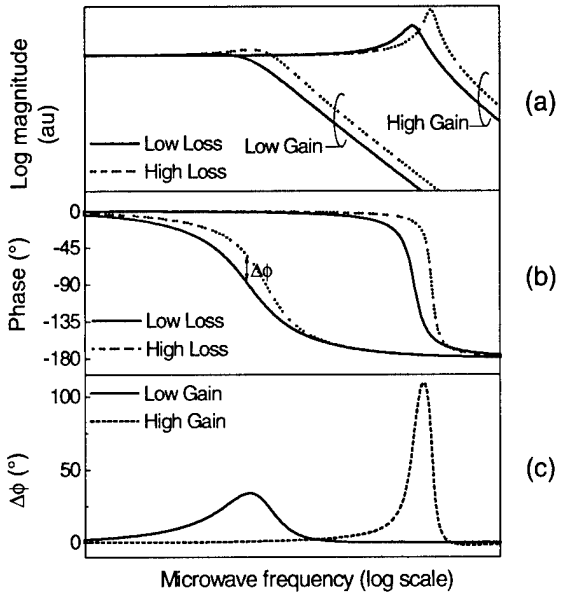

Figure 3.7. Schematic of the 2-pole small-signal modulation frequency response. a) Subcarrier amplitude; b) Subcarrier phase; c) Expected phase shift $\Delta\phi$ as absorber voltage is varied.

2.2.1 Experimental Results

Figure 3.8 shows the magnitude of the change in phase of the subcarrier as the absorber bias voltage is varied between 2V and -14V, for three different DC gain bias currents. These experimental results are in excellent agreement with the predictions of our model which are shown in Figure 3.7c. For each DC gain bias current, the phase shift is maximum when the subcarrier frequency coincides with the relaxation oscillation frequency, which increases as the square root of the current bias above threshold. Furthermore, as the gain bias current increases, the frequency range over which phase shifts occur narrows, as expected from Figure 3.7c.

With a standard two-contact laser such as that described by our simple two-pole model, the amplitude and phase responses of the subcarrier cannot be controlled independently of each other; see Figures 3.7a and 3.7b. However, our novel three-contact VCSEL, with separately biased gain and absorber regions, provides an extra degree of flexibility, allowing independent control of the subcarrier phase and magnitude. Figure 3.9 shows a contour plot for our device of the phase and magnitude of a 2.5 GHz optical subcarrier, as a function of the applied DC gain current and absorber bias voltage. The intersection of the magnitude contours with the phase contours demonstrates the ability to control the magnitude and phase independently. With this arrangement, we can obtain up to a 3.6dBm variation in the magnitude for a fixed phase of the subcarrier or we can vary the phase over 95° while maintaining a constant amplitude.

We have used this technique to demonstrate phase modulation of the optical subcarrier. With a DC gain bias ($I_{g,DC}$) of 7.3 mA, we apply to the gain contact (V_a) a 2 MHz, 5 V peak-to-peak square wave with a 5V DC offset. Under these conditions, the device operates at the two points shown in Figure 3.9; note that these two operating points have a constant amplitude but different phases. A time trace and the RF spectrum of the resulting phase-modulated optical subcarrier are shown in Figure 3.10. Analysis of the signal with a microwave vector signal analyzer shows that the phase-modulated component of this signal is more than 18 dB greater than the amplitude-modulated component.

Furthermore, this device can be used for simultaneous phase and amplitude modulation. The signal space which can be achieved using our device is shown in Figure 3.11. Ideally, all of the first-quadrant signal points for 16-QAM should fall within this achievable signal space; the other

three quadrants could then be obtained by applying standard 90° and 180° phase shifters to the microwave electrical drive current.

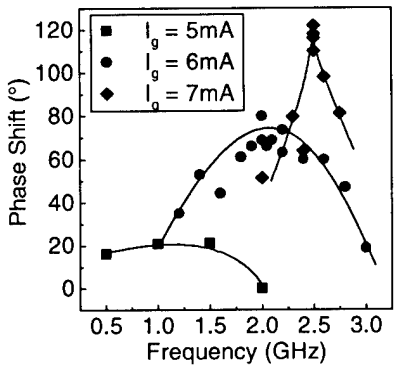

Figure 3.8. Measured subcarrier phase shift versus modulation frequency as absorber voltage is varied between 2V and –14V.

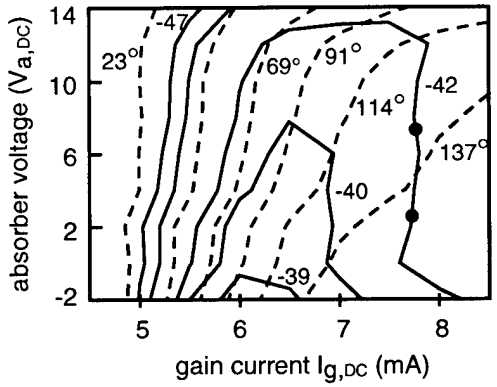

Figure 3.9. Contour plot of the measured phase and amplitude response of a 2.5 GHz optical subcarrier to tuning of the absorber bias voltage ($V_{a,DC}$) and the gain bias current ($I_{g,DC}$). Solid curves are surfaces of constant subcarrier amplitude (measured in dBm), and dashed curves are surfaces of constant subcarrier phase. Dots show operating points for phase modulation in Figure 3.10.

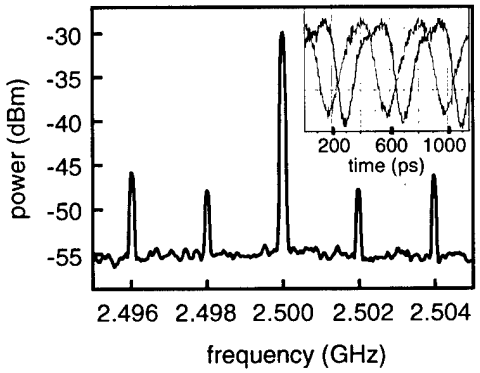

Figure 3.10. RF spectrum of phase modulation of the 2.5 GHz optical subcarrier. Inset shows phase-shifted time traces of the subcarrier. DC gain bias is 7.3mA; the electrical power of the applied modulation is -5dBm. A 5V peak-to-peak, 2 MHz square wave with a 5V DC offset is applied to the absorber.

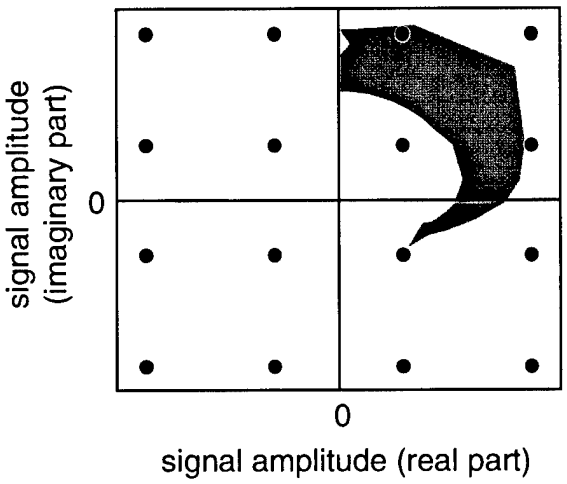

Figure 3.11. Achievable signal space which can be addressed using this device (gray region). Plot is overlaid with the signal points for 16-QAM.

3. Applications For Design B

3.1 Optical Bistability and Self-Pulsation

Self-pulsating lasers have a very short coherence length, rendering them highly insensitive to optical feedback. Hence, such devices have found extensive commercial use in applications such as optical disk readout. Self-pulsation has been demonstrated previously in edge-emitting lasers which use integrated active saturable absorbers to obtain controllable self-pulsations up to GHz frequencies. Recent work has focused on obtaining self-pulsating VCSELs because the surface normal geometry leads to advantages such as circular beam output and the potential for 2D arrays. Initial demonstrations of self-pulsation in VCSELs used defects caused by ion implantation as passive saturable absorbers; these efforts produced at most MHz range pulsations with RF linewidths of roughly 100 MHz [15, 16, 17]. Using our VCSEL with an intracavity absorber, we demonstrate for the first time self-pulsations which can be controlled by adjusting the voltage applied to the saturable absorber [18, 19]. The pulsations obtained using this technique can be turned on and off at will, and the frequency of the pulsations can be tuned by adjusting the electrical bias. Furthermore, this control of the self-pulsation conditions enables the user to compensate for processing or growth errors.

The sharp negative differential resistance which occurs in the absorber of Design B enables the user to select between three possible states of operation of the laser: standard CW operation, bistable operation, or self-pulsation. The bias circuitry shown in Figure 4.2 imposes a DC load on the absorber. For each choice of load (R and V_0), the device must operate at the intersection between the corresponding load line and the characteristic absorber I-V response, as shown in Figure 4.3. Thus, the user can select the operation state of the laser by adjusting the position of the absorber load line. For example, with the absorber bias load line shown in Figure 4.3, the absorber characteristic for each gain bias current intersects the load line at exactly one point. This choice of load results in the conventional output power versus current (L-I) response shown in Figure 4.2.

Because of the sharp negative differential resistance in the absorber characteristic, it is possible to select an absorber bias such that the load line intersects an absorber IV characteristic at three points, as shown in Figure 4.4. Two of these three intersections are stable operating points, so with this load the device operates in the bistable manner shown in Figure 4.5. By decreasing the bias resistance R, the user effectively increases the slope of the load line, which narrows the hysteresis eye of the bistable response [19].

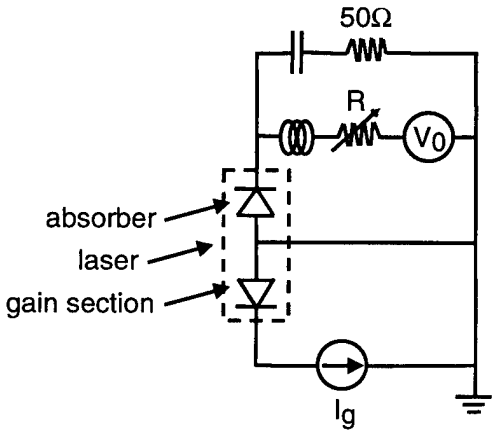

Figure 4.2. Biasing circuitry used to obtain bistability, self-pulsation, and optical pickup applications for Design B.

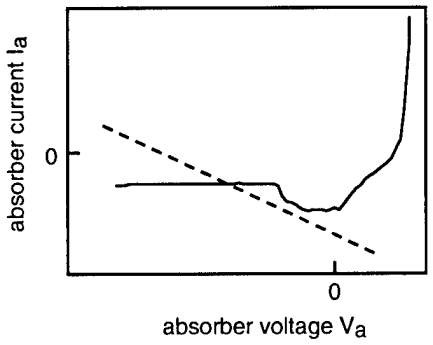

Figure 4.3. Solid line shows a schematic of the absorber current vs. voltage (I_a-V_a) characteristic. Dashed line shows a possible choice of absorber load line.

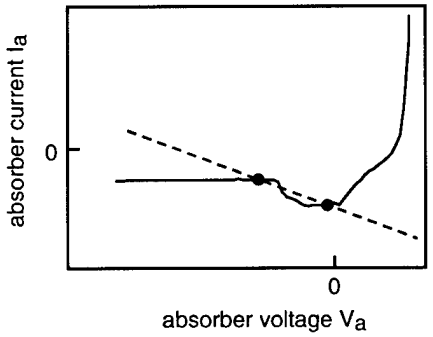

Figure 4.4. Bistable operation: the absorber is biased so that the operating load line (dashed line) intersects the absorber I_a-V_a trace (solid line) three times.

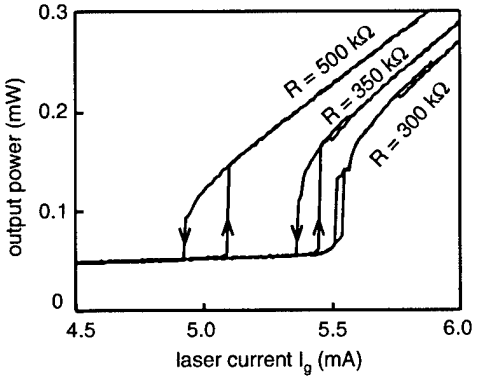

Figure 4.5. Bistable operation: the L-Ig trace exhibits a discontinuity in dL/dIg and a hysteresis loop. Absorber is biased with V_0 = 40V and R = 500 kΩ, 350 kΩ, or 300 kΩ.

Self-pulsation of Design B is achieved by adjusting the absorber bias conditions so that the operating load line is tangential to the region of negative differential resistance in the absorber I_a-V_a trace; see Figure 4.6. Because Design B is designed as discussed in Section 3 to obtain

regions of sharp negative differential resistance in the absorber I_a-V_a characteristic, relatively low absorber biases (R = 10-100 kΩ, V_0 = 5-15 V) are required to obtain self-pulsation. Furthermore, self-pulsation of the device can be obtained at a range of bias currents (I_g) and output powers by choosing R and V_0 so that the load line is tangential to the absorber I_a-V_a trace at the desired bias current. This unique feature is a particular strength of our device.

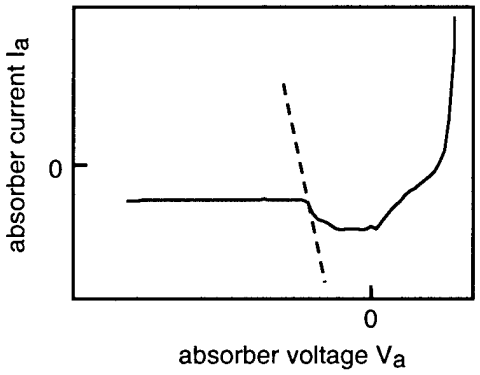

Figure 4.6. Self-pulsation regime: the absorber is biased so that the operating load line (dashed line) is tangential to the absorber I_a-V_a trace (solid line).

3.1.1 Experimental Demonstration of Self-Pulsation

With the Design Biased as shown in Figure 4.2, we measure the optical output using an RF spectrum analyzer. When the device is biased so that it does not self-pulsate, the RF spectrum shows only a broad peak due to relative intensity noise; see Figure 4.7. When the absorber bias conditions are adjusted such that the operating load line is tangential to the region of negative differential resistance in the absorber IV, the device

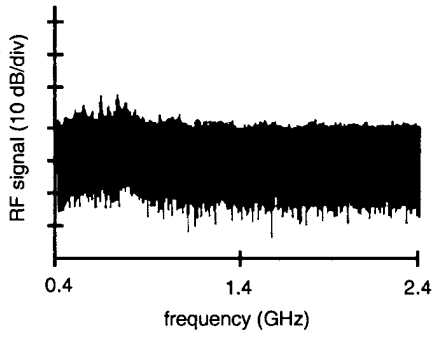

Figure 4.7. RF spectrum analyzer trace of the VCSEL output when the device is not biased for self-pulsation (R = 100 kΩ, V_0 = 10 V, I_g = 5.3 mA)

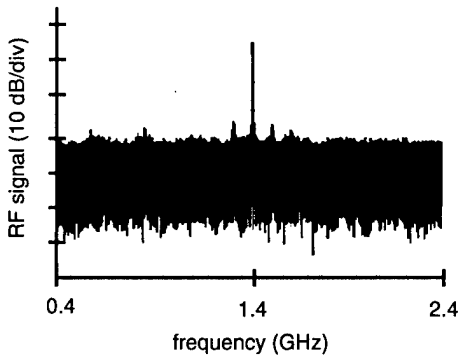

Figure 4.8. RF spectrum analyzer trace of the VCSEL output when the device is biased for self-pulsation (R = 75 kΩ, V_0 = 7 V, I_g = 6 mA)

self-pulsates at a GHz-range repetition rate, resulting in the sharp peak in the RF spectrum shown in Figure 4.8. The self-pulsation peak is roughly 40 dB above background.

As illustrated by the enlarged RF trace shown in Figure 4.9, the self-pulsation peak has an extremely narrow RF linewidth of 700 kHz, indicating that the pulsation frequency is remarkably stable. Furthermore, as expected, our device self-pulsates at the relaxation oscillation frequency of the laser, so the pulsation frequency can be tuned by adjusting the gain bias current (I_g). As the gain bias current is varied, the absorber load (R and V_0) must be adjusted so that the operating load line remains tangential to the absorber IV (see Figure 4.6) in order to maintain self-pulsation. Figure 4.10 shows tuning of the self-pulsation frequency over 700 MHz using this technique.

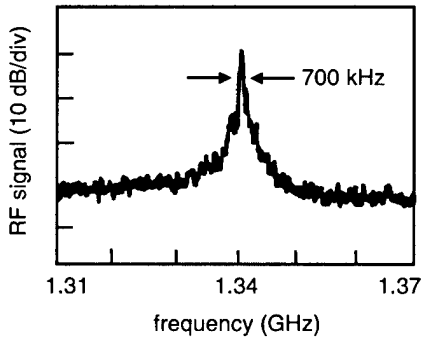

Figure 4.9. RF spectrum analyzer trace of the VCSEL output when the device is biased for self-pulsation (R = 75 kΩ, V_0 = 6 V, I_g = 6 mA)

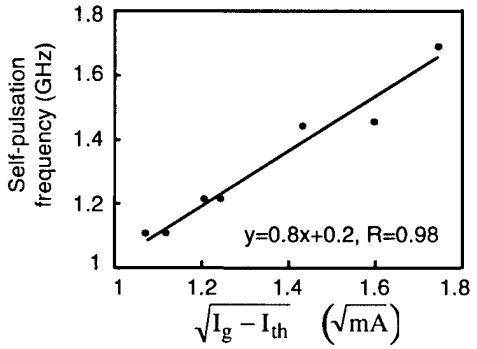

Figure 4.10. Tuning of the self-pulsation frequency with gain bias current (I_g). I_{th} is the threshold gain bias current at which the Design Begins to lase.

3.2 Optical Disk Readout

Conventional optical disk readout systems use an edge-emitting laser as the optical source and a separate external photodetector to monitor the light reflected from the optical disk. This arrangement requires the use of either a self-pulsating optical source or polarization rotators and beam splitters in order to minimize undesirable back-reflections from the external optics into the laser cavity. In addition, the highly asymmetric beam output of edge-emitting lasers requires precise optical lens design in order to maximize the allowable information density on the optical disk. An alternative approach is to integrate the photodetector with the optical source, as has been demonstrated previously with a double-contact, edge-emitting laser [14]. Such an arrangement offers a significant reduction in the size of the optical pick-up head and minimizes undesirable reflections.

We demonstrate a novel integrated optical disk readout head using our vertical-cavity, surface-emitting laser with an intracavity quantum-well absorber. The CW optical beam emitted by the VCSEL is tightly focussed onto the optical disk, and the reflected beam then propagates directly back into VCSEL cavity. Under reverse bias, the intracavity absorber functions as a photodetector, with the generated photocurrent providing an accurate measure of the variations in optical feedback due to the optical disk.

In a conventional VCSEL with no intracavity absorber, we would expect to see minimal change of the voltage across the laser in response to optical feedback, since the Fermi level of the gain region is clamped. However, by placing a separate intracavity quantum-well absorber into the mirror stack of our VCSEL, we obtain a substantial variation in the absorber photocurrent in response to optical feedback, even under lasing conditions. In addition, by exploiting the design flexibility and unique device physics of a VCSEL with an intracavity absorber in order to operate the device in an optically bistable manner, we are able to further magnify the readout signal obtained using our pickup head.

Several major advantages arise from our use of a vertical-cavity Design As an optical pickup head. First, the circular beam output can be tightly focussed, allowing very high density data storage on the optical disk. The extremely short cavity length of the surface-emitting laser results in single longitudinal lasing mode, thereby eliminating the intermodal noise that can arise in systems using edge-emitting lasers. Finally, the surface-normal geometry enables the construction of two-dimensional arrays of these devices, so our novel optical pickup head could potentially be used for parallel readout, vastly increasing the information bandwidth of the readout system.

The optical disk readout application is simulated by placing our device in an external optical cavity, as shown in Figure 4.11. The laser output beam is first collimated and then focussed onto a 95% reflecting mirror, which provides optical feedback into the device. A mechanical chopper placed in front of the mirror simulates low frequency optical disk readout. For actual disk readout, the mirror and chopper would be replaced with the optical disk.

The device is biased using the driving circuitry shown in Figure 4.12. The gain region is driven with a DC current source, while the absorber is biased using a DC voltage source (V_0) in series with a large resistance (R_1+R_2). A shunt capacitor is used to provide a termination path for any high frequency current generated in the absorber, while a blocking inductor isolates the DC voltage source V_0.

Typical absorber current versus voltage (I_a-V_a) traces for the device, with and without optical feedback from the external mirror, are shown in Figure 4.13. The DC absorber bias conditions (R_1+R_2 and V_0) are chosen so that the operating load line intersects the absorber I_a-V_a trace three times. For the case shown in Figure 4.13 (load line A), the absorber is biased with R_1+R_2=200 kΩ, V_0=9V. With this choice of load line, the device operates in a bistable manner, exhibiting a sharp discontinuity in the light versus current (L-I_g) curve as shown in Figure 4.14, along with a

corresponding hysteresis loop [17, 19]. The DC load R_1+R_2 is chosen to minimize the width of the hysteresis loop while maintaining as large a discontinuity in the L-I_g curve as possible.

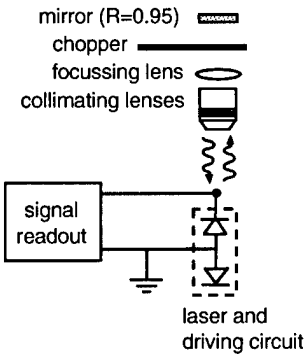

Figure 4.11. Experimental setup for optical disk readout application. The driving circuit is detailed in Figure 4.12.

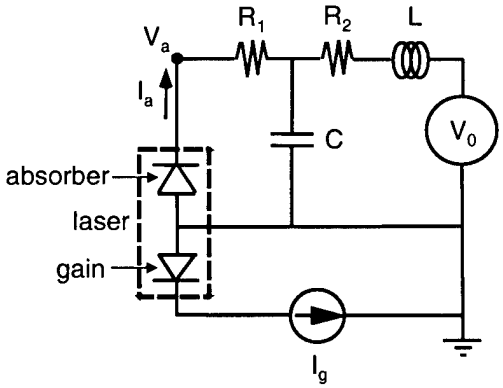

Figure 4.12. Biasing circuit for optical disk readout application.

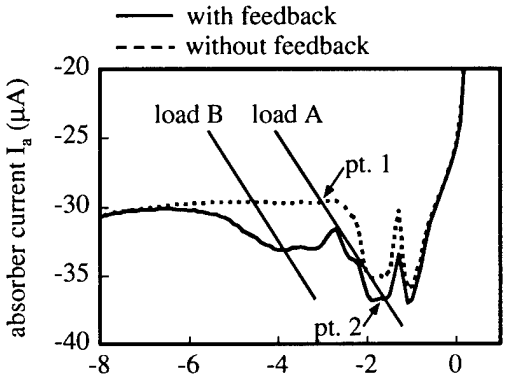

Figure 4.13. Absorber current versus voltage (I_a-V_a) with a fixed gain bias current I_g = 2.05 mA. Dotted line shows the response without optical feedback, and the solid line shows the response with optical feedback. Load line A corresponds to a DC absorber bias of R_1+R_2 = 200 kΩ, V_0 = 9 V. With this load and a gain current of I_g = 2.05 mA, the device operates at Point 1 (I_a = 29.62 μA) without optical feedback and at Point 2 (I_a = 36.64 μA) with optical feedback. Load line B illustrates operation of the device outside of the regime of sharp negative differential resistance.

Figure 4.14 shows the power versus current (L-I_g) trace for this device, both with and without optical feedback from the mirror. Without optical feedback, the laser threshold is I_{th1}=2.12 mA. Providing optical feedback effectively decreases the cavity loss, so the threshold decreases to I_{th2}=2.04 mA. Likewise, a similar response is observed in the absorber current versus laser bias current (I_a-I_g) traces, which are also shown in Figure 4.14.

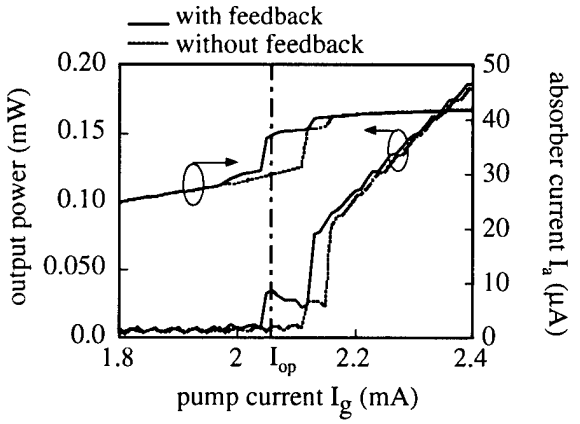

Figure 4.14. Output power versus gain bias current (L-I_g) and absorber current versus gain bias current (I_a-I_g). Dotted line shows the response without optical feedback, and the solid line shows the response with optical feedback. The backwards sweeps which complete the nearly closed hysteresis loops have been omitted for clarity. A typical gain bias point (I_{op}=2.05mA) used in the optical pickup measurements is shown by the dash-dot line. The DC absorber bias is R_1+R_2 = 200 kΩ, V_0 = 9 V.

For our optical pickup experiments, we bias the gain region at a value of I_{op} between I_{th1} and I_{th2}. As shown in Figure 4.14, this results in a dramatic increase in the output power of the device with optical feedback. The absorber photocurrent also increases with optical feedback, due to the absorption of increasing numbers of photons. With the laser biased between I_{th1} and I_{th2} (I_{op}=2.05 mA), the absorber current increases from I_a=29.62 μA without optical feedback to 36.64 μA with optical feedback.

3.2.1 Readout Results

Monitoring the resulting variations in the voltage V_a across the absorber provides a compact, integrated method of optical pickup detection. Figure 4.15 shows an oscilloscope trace of the absorber voltage with a chopper frequency of 2.5 kHz. The absorber voltage waveform has a 0.22 V peak-to-peak swing with a RC time constant of 20 μs. The measured signal-to-noise ratio is 10 dB at a chopper frequency of 1.5 kHz.

The measured 20 μs time constant corresponds to a roll-off frequency of 50 kHz, which is well beyond the range of the mechanical chopper. Further extending the bandwidth of the readout head will require detailed analysis of the electrical characteristics of our novel VCSEL, in conjunction with designing high speed bias circuitry. The intracavity absorber has been demonstrated to respond to modulation frequencies as high as 9 GHz and hence is not a limiting factor in the readout speed of the proposed optical head [6].

In addition to signal bandwidth, issues such as reduced optical feedback into the cavity, variations in the optical path length, and the choice of source wavelength arise in a practical optical disk readout system. The low reflectivity of an optical disk and possible beam truncation by the focussing lens can contribute to a substantial reduction in the optical feedback into the cavity. However, our robust optical disk readout head is remarkably insensitive to deliberate errors in focussing or alignment of the beam. Furthermore, variations of up to 1 cm in the optical path length do not alter the magnitude of the readout signal, so this device should be relatively insensitive to small mechanical variations, provided that the optical disk remains within the focal

plane of the beam. Finally, although our optical pickup head was demonstrated at a lasing wavelength of 960 nm, fabrication of the pickup head at shorter wavelengths requires no significant design changes [6, 11].

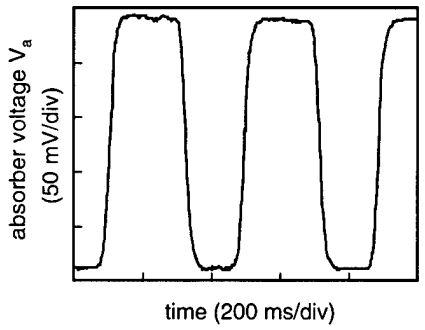

Figure 4.15. Experimentally observed oscilloscope time trace of the absorber voltage (V_a) in the presence of optical feedback modulated by a chopper at frequency 2.5 GHz. The bias conditions used are R_1 = 68 kΩ, R_2 = 112 kΩ, C = 0.2 μF, L = 10 H, V_0 = 9 V, I_g = 2.5 mA.

3.2.2 Signal Amplification

Figure 4.13 illustrates the effect of the absorber bias conditions on the variation observed in the absorber current with changes in optical feedback. By biasing the device to operate in a bistable manner so that the operating load line falls within the regime of negative differential resistance (Figure 4.13, load line A), the absorber current is 7 μA greater with optical feedback than without optical feedback. This result is observed both experimentally (ΔI_a=7.02 μA) and from Figure 2 (ΔI_a=7.1 μA). If instead the device is biased to operate outside of the NDR regime, we expect an absorber current variation of no more than 3 μA with feedback; see load line B in Figure 4.13. This magnification of the absorber current variation due to the NDR results in a large peak-to-peak swing in the monitored absorber voltage V_a as the pickup detection is performed. Hence, the design flexibility of our device enables us to achieve a signal amplification which is not available in a conventional photodetector, forming the basis for remarkably efficient optical pickup detection.

4. Impact And Recommendation For Future Work

We have demonstrated the first VCSEL with an integrated modulator/absorber section to perform a variety of novel functions. Indeed, we started an entire class of devices. The most intriguing part of this design is the possibility of separately engineer the lasing wavelength and absorption wavelength. With this independent control, which has never been achieved before with any other laser structures, we discovered a large number of device applications. We executed two distinct designs for our structures, leading to novel device physics and a wide range of applications, including low-chirp modulator-laser integration, QAM, bistable laser and self-pulsating laser.

This invention deserves more research work to fully exploit the opportunity brought forth by this new class of VCSELs we have started. In fact, other research organizations, e.g. Sandia National Labs and Tokyo Institute of Technology, have already followed our lead and published their new designs and inputs. We believe the impact of this work is an exceedingly far-reaching one.

Under this program, we graduated 3 PhD students, one post-doctoral researcher and one MS student. The grant also helped to start several new students. As the research scope became far wider than we initially anticipated, we are fortunate to be able to leverage the support from another ONR grant, MURI-RF Photonics program lead by UCLA. We published over 20 publications and presented about a dozen invited talks in international conferences.

We believe a wide avenue of device research has just been opened by this work. To just name a few examples of the future work, we recommend further studies on integrated modulators to establish chirp-engineering capability. This capability shall be made possible for the first time using this device structure. More work will be essential for high frequency RF photonics applications. Though it is difficult to design a VCSEL with linear light-current characteristics, with an integrated absorber, one shall be able to engineer a desirable LI curve to meet application needs.

5. Students Supported By This Program

Former students:	Sui F. Lim, PhD 1998 Now at Agilent
	W. Yuen, PhD 1999 Now at Bandwidth9 Inc.
	Rob Stone, Postdoc, 1999 Now at Bandwidth9 Inc.
	Janice Hudgings, PhD 1999 Now at Mount Holyoke College
	Steve Chase, MS 2000 Now at Johns Hopkins University
Current Students:	Lukas Chrostowski, Chih-Hao Chang, Jacob Hernadez, P. C. Ku

6. Publications

1) J.A. Hudgings, R.J. Stone, S.F. Lim, G.S. Li, W. Yuen, K.Y. Lau, and C.J. Chang-Hasnain, "The Physics of Negative Differential Resistance of an Intracavity Voltage-Controlled Absorber in a Vertical Cavity Surface Emitting Laser," Applied Physics Letters, 73 (13), p.1796-1798, 1998.

2) J.A. Hudgings, S.F. Lim, G.S. Li, W. Yuen, K.Y. Lau, and C.J. Chang-Hasnain, "Compact, Integrated Optical Disk Readout Head using a Novel Bistable Vertical Cavity Surface Emitting Laser," *Photonics Technology Letters*, 1998.

3) J.A. Hudgings, S.F. Lim, G.S. Li, W. Yuen, K.Y. Lau, and C.J. Chang-Hasnain, "Self-Pulsations, Bistability, and Intracavity Quantum Well Absorber Modulation of VCSELs," in *Optoelectronic Integrated Circuits II, Proceedings of the SPIE*, vol. 3290, ed. S. Wang and Y. Park, 1998.

4) J.A. Hudgings, R.J. Stone, C.H. Chang, S.F. Lim, K.Y. Lau, and C.J. Chang-Hasnain, "Dynamic Behavior and Applications of a Three-Contact Vertical Cavity Surface Emitting Laser," *IEEE Journal of Selected Topics in Quantum Electronics*, June, 1999.

5) R.J. Stone, J.A. Hudgings, C.H Chang, K.Y. Lau, and C.J. Chang-Hasnain, "Independent Phase and Magnitude Control of an Optically Carried Microwave Signal with a Three Terminal Vertical Cavity Surface Emitting Laser," *Photonics Technology Letters*, accepted for publication, 1998.

6) S.F. Lim, J.A. Hudgings, L.P. Chen, G.S. Li, W. Yuen, K.Y. Lau, and C.J. Chang-Hasnain, "Novel Intracavity Modulator Integrated with a Vertical-Cavity Surface-Emitting Laser," in *Trends in Optics and Photonics Series (TOPS)*, ed. C.J. Chang-Hasnain, Washington, D.C., Optical Society of America, 1997, vol. 15, p.48-52, 1997.

7) S.F. Lim, J.A. Hudgings, G.S. Li, W. Yuen, K.Y. Lau, and C.J. Chang-Hasnain, "Self-Pulsating and Bistable VCSEL with Controllable Intracavity Quantum-Well Saturable Absorber," *Electronics Letters*, 33 (20), p.1708-9, 1997.

8) S.F. Lim, J.A. Hudgings, L.P. Chen, G.S. Li, W. Yuen, K.Y. Lau, and C.J. Chang-Hasnain, "Modulation of a Vertical-Cavity Surface-Emitting Laser using an Intracavity Quantum-Well Absorber," *IEEE Photonics Technology Letters*, 10 (3), p.319-321, 1997.

9) S.F. Lim, J.A. Hudgings, G.S. Li, W. Yuen, K.Y. Lau, and C.J. Chang-Hasnain, "VCSELs with a Novel Integrated Quantum-Well Absorber," in *Vertical-Cavity Surface-Emitting Lasers II, Proceedings of the SPIE*, vol. 3286, ed. R.A. Morgan and K.D. Choquette, 1998.

10) S. F. Lim, G. S. Li, W. Yuen, and C. J. Chang-Hasnain, "Vertical Cavity Lasers with an Intracavity Quantum Well Detector," Electronics Letters, Vol. 33, 7, 27 March, 1997.

11) J.A. Hudgings, R.J. Stone, C.H Chang, K.Y. Lau, and C.J. Chang-Hasnain, "Integrated Phase and Magnitude Control of a Microwave Optical Subcarrier Using a Three-Contact Vertical Cavity Surface Emitting Laser with an Intracavity Absorber," (accepted), *1999 Optical Fiber Communication Conference*, San Diego, CA, February 1999.

12) J.A. Hudgings, S.F. Lim, R.J. Stone, G.S. Li, W. Yuen, K.Y. Lau, and C.J. Chang-Hasnain, "Applications and Device Physics of a Novel VCSEL with an Intracavity Quantum-Well Absorber," *OSA Annual Meeting*, Baltimore, MD, October 1998.

13) J.A. Hudgings, S.F. Lim, G.S. Li, W. Yuen, K.Y. Lau, and C.J. Chang-Hasnain, "Frequency Tuning of Self-Pulsations in a VCSEL with a Voltage-Controlled Saturable Absorber," *1998 Optical Fiber Communication Conference*, San Jose, CA, February 1998.

14) J.A. Hudgings, S.F. Lim, G.S. Li, W. Yuen, K.Y. Lau, and C.J. Chang-Hasnain, "Self-Pulsations, Bistability, and Intracavity Quantum Well Absorber Modulation of VCSELs," *SPIE Photonics West Optoelectronics Integrated Circuits Conference*, San Jose, CA, January 1998.

15) R.J. Stone, J.A. Hudgings, S.F. Lim, G.S. Li, K.Y. Lau, and C.J. Chang-Hasnain, "Negative Differential Resistance of an Intracavity Voltage-Controlled Absorber in a Vertical Cavity Surface Emitting Laser," 16th IEEE International Semiconductor Laser Conference, Nara, Japan, October 1998.

16) S. F. Lim, G. S. Li, W. Yuen, and C. J. Chang-Hasnain, "Intracavity Quantum-Well Photodetection of a Vertical-Cavity Surface-Emitting Laser," 15th IEEE International Semiconductor Laser Conference (ISLC'96), Haifa, Israel, 13-18 Oct. 1996.

17) S. F. Lim, L. P. Chen, G. S. Li, W. Yuen, K. Y. Lau, and C. J. Chang-Hasnain, "Novel Intracavity Modulator Integrated with a Vertical-Cavity Surface-Emitting Laser," Conference on Lasers and Electro-Optics (CLEO'97), Baltimore, MD, 18-23 May 1997, paper CWA3.

18) S.F. Lim, J.A. Hudgings, G.S. Li, W. Yuen, K.Y. Lau, and C.J. Chang-Hasnain, "Self-Pulsating VCSEL with Controllable Quantum-Well Saturable Absorber," *IEEE/LEOS'97 Summer Topical Meetings*, Montreal, Quebec, Canada, August 1997.

19) S.F. Lim, J.A. Hudgings, G.S. Li, W. Yuen, K.Y. Lau, and C.J. Chang-Hasnain, "Novel Bistable VCSEL for Efficient and Compact Optical Pickup Applications," *CLEO'98*, San Francisco, CA, May 1998.

20) S.F. Lim, J.A. Hudgings, G.S. Li, W. Yuen, K.Y. Lau, and C.J. Chang-Hasnain, "VCSELs with a Novel Integrated Quantum-Well Absorber," *SPIE Photonics West Optoelectronics Integrated Circuits Conference*, San Jose, CA, January 1998.

7. References

1 K. L. Lear, M. Ochiai, V. M. Hietala, H. Q. Hou, B. E. Hammons, J. J. Banas, and J. A. Nevers, "High-speed vertical cavity surface emitting lasers," presented at 1997 Digest of the IEEE/LEOS Summer Topical Meetings: Vertical Cavity Lasers, 1997.

2 F. S. Choa, Y. H. Lee, T. L. Kock, C. A. Burrus, B. Tell, J. L. Jewell, and R. E. Leibenguth, "High-speed modulation of vertical-cavity surface-emitting lasers," *Photonics Technology Letters*, vol. 3, pp. 697-699, 1991.

3 J. W. Scott, B. J. Thibeault, C. J. Mahon, L. A. Coldren, and F. H. Peters, "High modulation efficiency of intracavity contacted vertical cavity lasers," *Applied Physics Letters*, vol. 65, pp. 1483-1485, 1994.

4 S. F. Lim, J. A. Hudgings, L. P. Chen, G. S. Li, W. Yuen, K. Y. Lau, and C. J. Chang-Hasnain, "Novel intracavity modulator integrated with a vertical-cavity surface-emitting laser," presented at OSA TOPS: Advances in Vertical Cavity Lasers, 1997.

5 W. T. Tsang, J. E. Johnson, P. A. Morton, T. Tanbun-Elk, S. N. G. Chu, and W. D. Johnston, "Integrated laser/modulators for high capacity WDM transmission systems," *IEEE MTT-S Digest*, pp. 247-250, 1995.

6 S. F. Lim, J. A. Hudgings, L. P. Chen, G. S. Li, W. Yuen, K. Y. Lau, and C. J. Chang-Hasnain, "Modulation of a vertical-cavity surface-emitting laser using an intracavity quantum-well absorber," *IEEE Photonics Technology Letters*, vol. 10, pp. 319-321, 1997.

7 L. A. Coldren and S. W. Corzine, *Diode Lasers and Photonic Integrated Circuits.* New York: Wiley, 1995.

8 D. A. Cohen, Y. Chang, A. F. J. Levi, H. R. Fetterman, and I. L. Newberg, "Optically controlled serially fed phased array sensor," *IEEE Photonics Technology Letters*, vol. 8, pp. 1683-1685, 1996.

9 Y. Chang, B. Tsap, H. R. Fetterman, D. A. Cohen, A. F. J. Levi, and I. L. Newberg, "Optically controlled serially fed phased-array transmitter," *IEEE Microwave and Guided Wave Letters*, vol. 7, pp. 1069-1071, 1997.

10 B. Tsap, Y. Chang, H. R. Fetterman, A. F. J. Levi, D. A. Cohen, and I. Newberg, "Phased-array optically controlled receiver using a serial feed," *IEEE Photonics Technology Letters*, vol. 10, pp. 267-9, 1998.

11 J. A. Hudgings, R. J. Stone, S. F. Lim, G. S. Li, W. Yuen, K. Y. Lau, and C. J. Chang-Hasnain, "The physics of negative differential resistance of an intracavity voltage-controlled absorber in a vertical cavity surface emitting laser," *Applied Physics Letters*, vol. 73, pp. 1796-1798, 1998.

12 P. J. Anthony, T. L. Paoli, and R. L. Hartman, "Observations of negative resistance associated with superlinear emission characteristics of (Al,Ga)As double-heterostructure lasers," *IEEE Journal of Quantum Electronics*, vol. 16, pp. 735-739, 1980.

13 J. P. van der Ziel, "Time-dependent voltage measurement of pulsating AlxGa1-x double-heterostructure lasers," *Applied Physics Letters*, vol. 35, pp. 116-118, 1979.

14 C. Harder, K. Y. Lau, and A. Yariv, "Bistability and pulsations in semiconductor lasers with inhomogeneous current injection," *IEEE Journal of Quantum Electronics*, vol. 18, pp. 1351-1361, 198

15 K. D. Choquette, H. Q. Hou, K. L. Lear, H. C. Chui, K. M. Geib, A. Mar, and B. E. Hammons, "Self-pulsing oxide-confined vertical-cavity lasers with ultralow operating current," *Electronics Letters*, vol. 32, pp. 459-460, 1996.

16 D. G. H. Nugent, R. G. S. Plumb, M. A. Fisher, and D. A. O. Davies, "Self-pulsations in vertical-cavity surface-emitting lasers," *Electronics Letters*, vol. 31, pp. 43-44, 1995.

17 X. Tang, J. P. van der Ziel, B. Chang, R. Johnson, and J. Tatum, "Observation of bistability in GaAs quantum-well vertical-cavity surface-emitting lasers," *IEEE Journal of Quantum Electronics*, vol. 33, pp. 927-932, 1997.

18 J. A. Hudgings, S. F. Lim, G. S. Li, W. Yuen, K. Y. Lau, and C. J. Chang-Hasnain, "Frequency tuning of self-pulsations in a VCSEL with a voltage-controlled saturable absorber," presented at Optical Fiber Communication Conference, San Jose, CA, 1998.

19 S. F. Lim, J. A. Hudgings, G. S. Li, W. Yuen, K. Y. Lau, and C. J. Chang-Hasnain, "Self-pulsating and bistable VCSEL with controllable intracavity quantum-well saturable absorber," *Electronics Letters*, vol. 33, pp. 1708-9, 1997.